

Modelling of transport and recombination of photocarriers in un-doped hydrogenated amorphous silicon (a-Si:H)

Souad Tobbeche* and Amar Merazga

Laboratoire des Matériaux Semiconducteurs et Métalliques
Université Mohamed Khider , B.P. 145, 07000 Biskra, Algeria

(reçu le 29 Mars 2006 - accepté le 25 Mars 2007)

Abstract - In this paper, we report on the simulation of steady state photoconductivity in un-doped a-Si:H at temperatures from 30 to 500 K. The model is based on recombination at dangling bond states and band tail states. It takes also into account the hopping transitions in the conduction band tail states to describe the conduction in localized states at low temperatures. At high temperatures, the multiple trapping process is considered to describe the conduction in extended states. The density of states includes the exponential density of conduction band tail states and valence band tail states and the density of dangling bond states. This later is determined by the Defect Pool Model 'DPM'. The experimental features observed on the temperature dependence of the photoconductivity (σ_p) are generally the thermal quenching, the low activated region and the temperature independent photoconductivity at very low temperatures. All these observations are well reproduced by the model in un-doped a-Si:H. By the examination of the relative contributions of two processes of conduction: (i) the multiple trapping and (ii) the multiple trapping associated with the hopping, the model results show that the multiple trapping process of electrons where the conduction is assured by free carriers in the thermal quenching region above 140 K is important while the hopping process of electrons is negligible. At 140 K and below, the hopping transport of electrons in the conduction band tail states makes an important contribution in the photoconductivity. It explains successfully the low activated region and the temperature independent photoconductivity at very low temperatures.

Résumé - Ce travail est une étude par simulation numérique de la dépendance de la photoconductivité en régime stationnaire de la température du a-Si:H intrinsèque dans un intervalle de température [30 K - 500 K]. Le modèle est basé sur la recombinaison dans les états des liaisons pendantes et les états de queues de bandes. Il prend aussi en considération les transitions par saut dans les états de queue de bande de conduction pour décrire la conduction dans les états localisés aux températures basses. Aux températures élevées, le processus de multi piégeage est considéré pour décrire la conduction dans les états étendus. La densité des états inclut la densité des états de queue de bande de conduction et de valence de formes exponentielles et la densité des états des liaisons pendantes. Cette dernière est déterminée par le Modèle Defect Pool 'MDP' de formation des défauts. Les caractéristiques généralement observées sur la dépendance en température de la photoconductivité (σ_p) sont le thermal quenching, la région thermiquement activée par une faible énergie et la photoconductivité indépendante de la température aux températures très basses. Toutes ces observations sont bien reproduites par le modèle dans le a-Si:H intrinsèque. Par l'examen des contributions relatives de deux processus de conduction: (i) le multi piégeage et (ii) le multi piégeage associé au processus par saut, les résultats du modèle montrent que le processus de multi piégeage d'électrons où la conduction qui est assurée par les porteurs libres dans la région du thermal quenching est prédominant, cependant, le processus de conduction par saut est négligeable à $T > 140$ K. A $T \leq 140$ K, le transport par saut d'électrons dans les états de queue de bande de conduction a une contribution importante dans la photoconductivité. Il explique avec succès la région faiblement activée et la photoconductivité indépendante de la température aux températures très basses.

Keywords: Silicium amorphe hydrogéné 'a-Si:H' - Steady state photoconductivity - Hopping - Density of states 'DOS'.

*Souad_tobbeche@yahoo.fr

1. INTRODUCTION

The study of the temperature dependence of the a-Si:H photoconductivity determines the different transport mechanisms, conduction at extended states and conduction by hopping through localized band tail states. The temperature dependence of the photoconductivity appears to have four regions [1-5]; the very low temperature region where the photoconductivity is nearly constant, the low and intermediate temperature region where the photoconductivity rises with temperature by several orders of magnitude, the high temperature region where the photoconductivity decreases with increasing temperature known as thermal quenching and finally, the higher temperature region where the photoconductivity increases rapidly with temperature.

Many models have been developed to explain the observed features of the photoconductivity in a-Si:H [6-9]. These models are distinguished from each other by the electronic structure and by the recombination mechanism, and use the Simons-Taylor theory [10] which neglected conduction by hopping among localized states and hence, the conduction is only in extended states. Each of the above models explains only some but not all the experimental results. The agreement between experiment and models is excellent in the high temperature regions. However the models and experimental results diverge in the middle and low temperature regions. All these simulation models have not considered the electron conduction by hopping in the localized states. According to Cloude, Spear *et al.* and Johanson [11-13], the hopping contribution to the steady state photoconductivity takes place at the low temperature range which is near 100 K and below. It is possible that both mechanisms contribute to the photoconductivity: conduction by free carriers in the extended conduction and valence band states and electron hopping through the localized states.

Shklovskii, Fritzsche and Baranovskii [14] have developed a theory to explain the very low temperature photoconductivity in which geminate recombination and energy loss hopping through localized states were considered. The very low temperature region was successfully explained by this theory. Monroe and Baranovskii *et al.* have also developed a theory in the low temperature region [15, 16]. They explain the rise of the photoconductivity with the temperature by a transport energy, E_t , where the hopping conduction contribution is maximum. With increasing temperature, E_t moves upward into more shallow localized states. The upward hops of electrons to the vicinity of E_t determine the transport.

The primary purpose of this work is to give some insight in which the transport model, of either through extended states or by hopping in localized states, reproduces approximately all the observed experimental behaviour of the a-Si:H steady state photoconductivity.

2. DENSITY OF STATES

The density of states ‘DOS’ used in the model includes exponential distributions attributed to the conduction band tail and to the valence band tail which are given by:

$$g_c(E) = G_c \exp\left(-\frac{E_c - E}{kT_c}\right) \quad (1)$$

$$g_v(E) = G_v \exp\left(-\frac{E - E_v}{kT_v}\right) \quad (2)$$

where k is the Boltzmann constant, E_c and E_v are the conduction and valence band edge energies, G_c and G_v are the band edge densities of states and T_c and T_v are the characteristic absolute temperatures of the conduction and valence band tail, respectively.

The density of the defect states $D(E)$ related to the density of the dangling bond states is developed according to the last version of the defect pool model [17-19]. The defect states density $D(E)$ expression is as follows:

$$D(E) = \xi \left(\frac{2}{f^0(E)} \right)^{kT^*/2E_{v0}} P \left(E + \frac{\sigma^2}{2E_{v0}} \right) \quad (3)$$

with

$$\xi = \left(\frac{G_v 2 E_{v0}^2}{(2 E_{v0} - kT^*)} \right) \left(\frac{H}{N_{SiSi}} \right)^{kT^*/4E_{v0}} \exp \left(\frac{-1}{2 E_{v0}} \left(E_p - E_v - \frac{\sigma^2}{4E_{v0}} \right) \right) \quad (4)$$

In equation (3), $P(E)$ is the defect pool of a Gaussian form with σ and E_p its width and peak position in the gap, T^* is the equilibrium temperature (freeze-in temperature) for which the density of states is maintained, $E_{v0} = kT_v$ is the width of the exponential valence band tail. H and N_{SiSi} are the total concentration of hydrogen and the total concentration of electrons in the material respectively.

The density of the defect states $D(E)$ divided into components of different charge densities that can be neutral (D^0), positively charged (D^+) or negatively charged (D^-) if occupied by zero, one, or two electrons, respectively are defined by:

$$D^+(E) = D(E) f^+(E) \quad (5a)$$

$$D^0(E) = D(E) f^0(E) \quad (5b)$$

$$D^-(E) = D(E) f^-(E) \quad (5c)$$

The occupation functions $f^+(E)$, $f^0(E)$ and $f^-(E)$ of dangling bond states D^+ , D^0 and D^- are given by [18]:

$$f^+(E) = \frac{1}{1 + 2 \exp([E_f - E]/kT) + \exp([2E_f - 2E - U]/kT)} \quad (6a)$$

$$f^0(E) = 2 \exp([E_f - E]/kT) f^+(E) \quad (6b)$$

$$f^-(E) = \exp([2E_f - 2E - U]/kT) f^+(E) \quad (6c)$$

The dark Fermi level E_f position in the gap is determined by considering the charge neutrality condition, involving all the densities of free, trapped carriers and the dangling bond occupancies.

Table 1 lists the parameters of the simulated dangling bond and the valence band tail densities, which are within the range of the published values in the literature [19]. For the simulated conduction band tail density parameters, the values of G_c and T_c have been chosen according to references [20] and [21], respectively.

Figure 1 shows the density of states distribution for un-doped a-Si:H. Because the density of dangling bond states $D(E)$ is dependant on the Fermi level E_f which is situated at the middle of the gap in un-doped a-Si:H. This makes the density of states distribution symmetric about the D^0 peak.

Table 1: Parameters used for the density of states calculation

Parameters		Value
G_v	$(\text{cm}^{-3}.\text{eV}^{-1})$	10^{21}
G_c	$(\text{cm}^{-3}.\text{eV}^{-1})$	$7 \cdot 10^{21}$
T_v	(K)	650
T_c	(K)	210
T^*	(K)	500
E_g	(eV)	1.9
E_{v0}	(meV)	56
$E_c - E_p$	(eV)	0.63
σ	(eV)	0.19
N_{SiSi}	(cm^{-3})	$2 \cdot 10^{23}$
H	(cm^{-3})	$5 \cdot 10^{21}$
U	(eV)	0.2

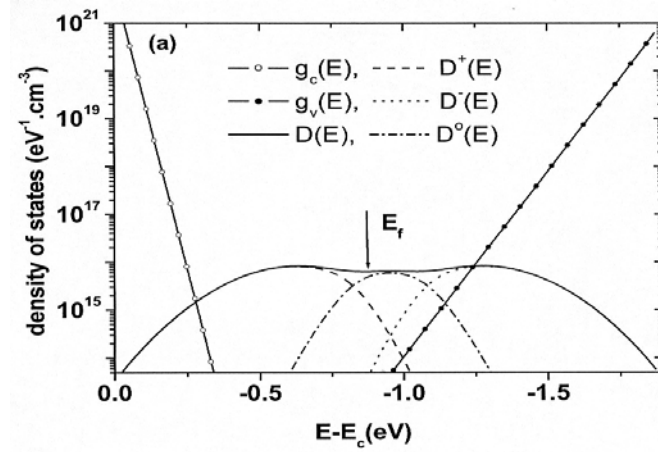


Fig. 1: Schematic illustration of the density of states in un-doped a-Si:H

3. STEADY STATE RATE EQUATIONS

Figure 2 shows schematically the conduction band tail state density $G_c(E)$, the valence band tail state density $G_v(E)$ and the dangling bond state density with three possible charge states represented, respectively $D^0(E)$, $D^+(E)$ and $D^-(E)$.

The arrows represent the recombination and the hopping paths. There are three possible recombination paths where the direct capture of free electrons and holes may take place; in the conduction band tail states, in the dangling bond states and in the valence band tail states. In regard of the hopping path, two transitions at the energy levels E_i and E_j schematise the hop up of electrons from E_i to E_j and the hop down of electrons from E_j to E_i . G is the generation rate of free carriers under continuous illumination.

The rate equations which describe the mechanism of transport in the steady state are the continuity equations for electrons and holes (equations (7) and (12), and the multiple trapping equations (equations (8), (9), (10) and (11)).

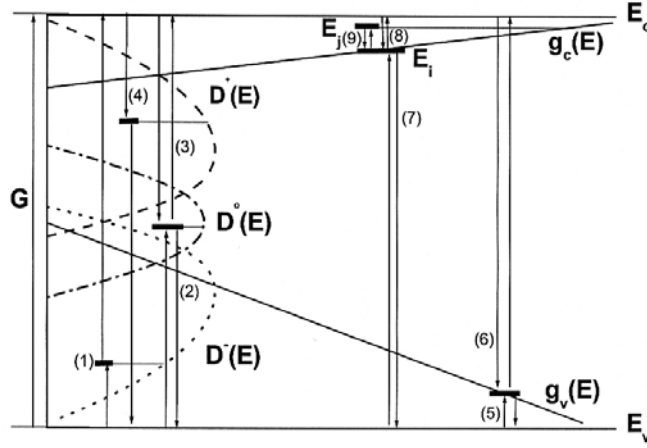


Fig. 2: Density of states and representation of the electron and hole transitions

(1): hole capture and electron emission by D^- states; (2): hole capture and electron emission by D^0 states; (3): electron capture and emission by D^0 states; (4): electron capture and emission by D^+ states; (5): hole capture and emission by g_v states; (6): electron capture and emission by g_v states; (7): hole capture and emission by g_c states; (8): electron capture and emission by g_c states and (9): electron hopping.

The rate equations at different transition levels can be written as:

$$\frac{dn}{dt} = 0 = -n \left(\sum_i C_n^c (N_{ti}^c - n_i) + \sum_i C_n^0 (N_{dbi} - N_i^- - N_i^+) + \sum_i C_n^+ N_i^+ + \sum_i C_n^v p_i \right) + \sum_i C_n^c n_i(i) n_i + \sum_i C_n^0 n_i^0(i) N_i^- + \sum_i C_n^0 n_i^0(i) (N_{dbi} - N_i^- - N_i^+) + \sum_i C_n^v n_i(i) (N_n^v - p_i) + G \quad (7)$$

$$\frac{dn_i}{dt} = 0 = \underbrace{n C_n^c (N_{ti}^c - n_i) - C_n^c n_i(i) n_i - C_p^c n_i p + C_p^c p_i(i) (N_{ti}^c - n_i)}_{(1)} + \underbrace{\left(\frac{N_{ti}^c}{G_T} \right) \sum_j n_j \Gamma_{i,j}}_{(2)} - \underbrace{n_i \sum_j \frac{N_{tj}^c}{G_T} \Gamma_{i,j}}_{(3)} \quad (8)$$

$$\frac{dN_i^-}{dt} = 0 = n C_n^0 (N_{dbi} - N_i^- - N_i^+) + C_p^0 p_i^0(i) (N_{dbi} - N_i^- - N_i^+) - C_n^0 n_i^0(i) N_i^- - C_p^- N_i^- p \quad (9)$$

$$\frac{dN_i^+}{dt} = 0 = p C_p^0 (N_{dbi} - N_i^- - N_i^+) + C_n^0 n_i^0(i) (N_{dbi} - N_i^- - N_i^+) - C_p^0 p_i^0(i) N_i^+ - C_n^+ N_i^+ n \quad (10)$$

$$\frac{dp_i}{dt} = 0 = p C_p^v (N_{ti}^v - p) + C_n^v n_i(i) (N_{ti}^v - p_i) - C_p^v p_i(i) p_i - C_p^v p_i n \quad (11)$$

$$\frac{dp}{dt} = 0 = G - p \left(\sum_i C_p^c n_i + \sum_i C_p^- N_i^- + \sum_i C_p^0 (N_{dbi} - N_i^- - N_i^+) + \sum_i C_n^v (N_{ti}^v - p_i) \right) + \sum_i C_p^c p_i(i) (N_{ti}^c - n_i) + \sum_i C_p^0 p_i^0(i) (N_{dbi} - N_i^- - N_i^+) + \sum_i C_p^0 p_i^0(i) N_i^+ + \sum_i C_p^v p_i(i) p_i \quad (12)$$

In addition, we have the charge neutrality equation written as:

$$-n - \sum_i n_i - \sum_i N_i^- + p + \sum_i p_i + \sum_i N_i^+ = 0 \quad (13)$$

The different notations used in the above equations: n , p are the free electron and hole densities; n_i , p_i are the trapped electron and hole densities on the level i of the conduction band tail states $g_c(E)$ and the valence band tail states $g_v(E)$; N_i^- , N_i^+ the negative and positive charge dangling bond states on the level i are $D^-(E_i).dE$ and $D^+(E_i).dE$; N_{ti}^c , N_{ti}^v the densities of the level i are $g_c(E_i).dE$ and $g_v(E_i).dE$; N_{dbi} the density of the level i is $D(E_i).dE$; G is the optical generation rate; $G_T = \sum_i N_{ti}^c$ is the total density of conduction band tail states; C_n^c , C_p^c are the capture coefficients of electrons and holes in the conduction band tail states; C_n^v , C_p^v are the capture coefficients of electrons and holes in the valence band tail states; C_n^+ , C_p^- are the capture coefficients of electrons and holes by the dangling bond states D^+ and D^- ; C_n^0 , C_p^0 are the capture coefficients of electrons and holes by the dangling bond D^0 . $n_1(i)$, $p_1(i)$ are the electron (hole) emission factors from the level i and $n_1^0(i)$, $p_1^0(i)$ are the electron (hole) emission factors to the conduction (valence) band from the defect state D^0 .

Equation 8 describes: (1) the carrier multiple trapping process performed by carrier capture and release by the conduction band tail states, (2) the hop in the level i from another localized level and (3) the hop of electrons out to another localized level [22]. The hopping process theory of amorphous semiconductors is just applied to the nearest neighbours of a given state [23]; that is the electron jumps to its nearest neighbour via tunnelling between an initial state located at the energy level E_i and a target state located at the energy level E_j . The term $\Gamma_{i,j}$ is the hopping rate from a state of energy E_i to another state of energy E_j over the distance $R_{i,j}$, it is described by the Miller and Abraham expression [24]:

$$\Gamma_{i,j} = v_o \exp\left(-\frac{2R_{i,j}}{a}\right) \times \begin{cases} \exp\left(-\frac{E_j - E_i}{kT}\right) & \text{hop up for } (E_j > E_i) \\ 1 & \text{hop down for } (E_j \leq E_i) \end{cases} \quad (14)$$

where v_o is the attempt to escape frequency and a is the localization radius of the localized conduction band tail states. $R_{i,j}$ is the hop distance from energy E_i to energy E_j . For an electron in a tail state at energy E_i , the downward hop distance $R_{i,j}$, of this electron to a neighbouring localized state at energy, $E_j \leq E_i$ has the following expression [16]:

$$R_{i,j} = \left\{ (4\pi/3) \int_{E_v}^{E_i} g_c(x) dx \right\}^{-1/3} \quad (15)$$

The upward hop distance $R_{i,j}$ of this electron to a neighbouring localized state at energy, $E_j > E_i$, is defined by:

$$R_{i,j} = \left\{ (4\pi/3) \int_{E_v}^{E_v} g_c(x) dx \right\}^{-1/3} \quad (16)$$

In equation (8), the terms (2) and (3) contain summations over all j including $j = i$. It should be noted that the rate equations (7)-(12) form non linear system. This is numerically solved by the Newton Raphson method where n , p , n_i , p_i , N_i^- , N_i^+ are evaluated for each value of temperature.

The total hopping photoconductivity (σ_{hop}) is obtained by the application of the Einstein relation, σ_{hop} is evaluated by summation over all the levels i [22]:

$$\sigma_{hop} = \frac{e^2}{6kT} \sum_i (R_{i,j})^2 n_i v_i \quad (17)$$

v_i is equivalent to the probability per second of a carrier jumping out of the level i and is given by [22]:

$$v_i = v_o \sum_j \frac{N_{ij}^c}{G_T} \exp\left(-\frac{2R_{i,j}}{a}\right) \exp\left(-\frac{E_j - E_i}{kT}\right) \quad (18)$$

In the multiple trapping mechanism, the free electron and hole in conduction and valence bands contribute to the photoconductivity by the known relation:

$$\sigma_{mt} = e(\mu_n n + \mu_p p) \quad (19)$$

where μ_n (μ_p) is the electron (hole) mobility in the conduction (valence) band and e is the electron charge.

When the multiple trapping and hopping processes occur simultaneously, the whole photoconductivity (σ_p) is simply the sum of equation (17) and (19):

$$\sigma_p = \sigma_{mt} + \sigma_{hop} \quad (20)$$

Table 2 lists the parameter values used in our simulation which are those mostly referred to in the literature: The values of the different recombination coefficients are taken from reference [21]. The mobility's for electrons and holes are respectively, $\mu_n = 10 \text{ cm}^2 \cdot \text{s}^{-1} \cdot \text{V}^{-1}$ [12, 25] and $\mu_p = 0.3 \text{ cm}^2 \cdot \text{s}^{-1} \cdot \text{V}^{-1}$ [12]. The attempt to escape frequency v_o was taken equal to $2 \cdot 10^{11} \text{ s}^{-1}$ which is close to the communally used value ($v_o = 10^{12} \text{ s}^{-1}$) and the localization radius of the order $a = 10^{-7} \text{ cm}$ [26].

Table 2: Parameters used for the photoconductivity calculation

Parameters		Value
$(N_c = N_v)$	(cm^{-3})	10^{20}
$(C_n^0 = C_p^0)$	$(\text{cm}^{-3} \cdot \text{s}^{-1})$	$5 \cdot 10^{-8}$
$(C_n^+ = C_p^-)$	$(\text{cm}^{-3} \cdot \text{s}^{-1})$	$5 \cdot 10^{-7}$
$(C_n^c = C_p^v)$	$(\text{cm}^{-3} \cdot \text{s}^{-1})$	$5 \cdot 10^{-8}$
$(C_p^c = C_n^v)$	$(\text{cm}^{-3} \cdot \text{s}^{-1})$	$5 \cdot 10^{-9}$
μ_n	$(\text{cm}^2 \cdot \text{s}^{-1} \cdot \text{V}^{-1})$	10
μ_p	$(\text{cm}^2 \cdot \text{s}^{-1} \cdot \text{V}^{-1})$	0.3
v_o	(s^{-1})	$2 \cdot 10^{11}$
a	(cm)	10^{-7}

4. RESULTS AND DISCUSSIONS

Figure 3 shows the modelled temperature dependence of the normalized photoconductivity σ_p / eG for $G = 10^{20} \text{ cm}^{-3} \cdot \text{s}^{-1}$ over a range extending from 30 to 500 K. From the figure, we can distinguish four regions:

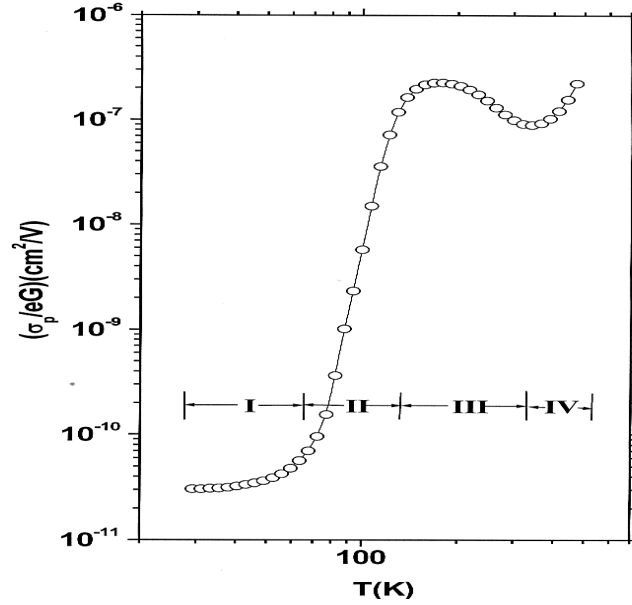


Fig. 3: Temperature dependence of the normalized photoconductivity in un-doped a-Si:H for $G = 10^{20} \text{ cm}^{-3} \cdot \text{s}^{-1}$

Region I

This region corresponds to very low temperatures. The normalized photoconductivity is very small and nearly constant; it has the value of $3 \cdot 10^{-11} \text{ cm}^2/\text{V}$.

Region II

This region covers the range of low and intermediate temperatures. The normalized photoconductivity highly increases by several orders of magnitude and has a thermally activated behaviour with a small activation energy ($E_a = 0.12 \text{ eV}$).

Region III

This region corresponds to high temperatures which includes the maximum and the minimum of the photoconductivity. This curve shows the thermal quenching; a region in which the photoconductivity decreases with increasing temperature.

Region IV

This region corresponds to very high temperatures. In this region also, there is an increase in the photoconductivity with temperature.

Figure 4 shows the temperature dependence of the normalized photoconductivity in un-doped a-Si:H for $G = 10^{20} \text{ cm}^{-3} \cdot \text{s}^{-1}$. Curve A shows $\sigma_p(T)$ calculated with modelling solely the multiple trapping process and neglecting the hopping process. The hopping terms in the rate equation (8) can be zeroed by taking the attempt to escape frequency ν_0 equal to zero. In this case, σ_p is due only to free electron and hole conduction in the conduction and in the valence

bands by multiple trapping process. However, curve B shows $\sigma_p(T)$ calculated with modelling the hopping and the multiple trapping processes which occur simultaneously. In curve A, the model explains just some of the experimental resultants but not all. For example, the model provides the thermal quenching region III and the region IV in Fig. 3, however, in the region II, the activation energy (E_a) of the calculated dependence $\log \sigma_p(1/T)$ is 0.03 eV which is less than that of the dependence $\log \sigma_p(1/T)$ obtained experimentally ($E_a = 0.11$ eV) [1, 3-5]. Furthermore, the constant behaviour of σ_p in region I of Fig. 3 proved experimentally [1-5] disappears in this case. In curve B, it appears clearly that the model describes, in a self consistent way, all the features observed for the temperature dependence of the photoconductivity in a-Si:H [1-5]. The most important results are the constant magnitude of $(\sigma_p / eG = 3 \cdot 10^{-11} \text{ cm}^2 / \text{V})$ in region I and the increase of σ_p by several orders of magnitude in region II with an activation energy ($E_a = 0.12$ eV) [5]. Curve A and B are superposed at temperatures ($T > 140$ K), in this range of temperature, both curves show an excellent agreement with the experimental results mentioned in references [1-5]; the conduction is carried by the free electrons and holes through the conduction and valence bands and according the multiple trapping transport process. In this case, the effect of the hopping on the photoconductivity is not pronounced.

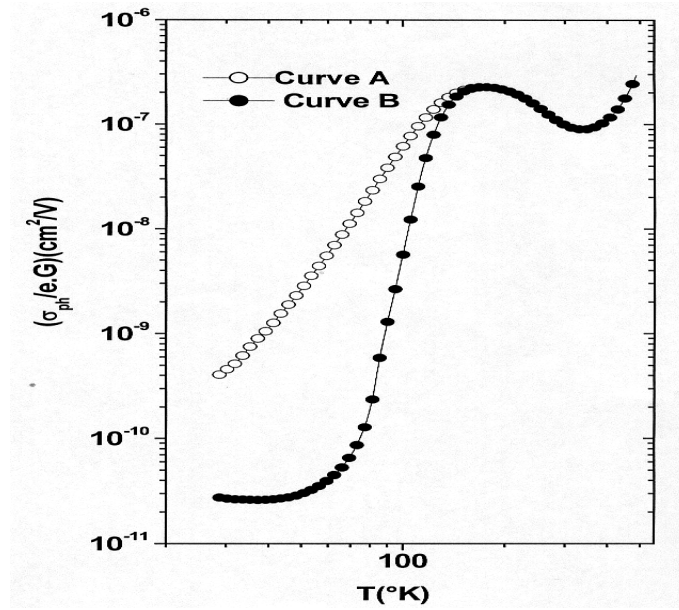


Fig. 4: Temperature dependence of the normalized photoconductivity in un-doped a-Si:H for $G = 10^{20} \text{ cm}^{-3} \text{ s}^{-1}$

Shklovskii *et al.* [14] developed a theory to explain $\sigma_p(T)$ in the very low temperature region (region I). The theoretical expressions of σ_p / eG is written [14] as:

$$\frac{\sigma_p}{eG} = 0.6 \frac{e a^2 L^2}{k T_c} \quad (21)$$

where L is the solution of equation $L = \ln \left[G \tau_0 (a L)^3 \right]^{-1}$ and it represents the average separation of photocarriers in units of a . τ_0 the dipole radiative lifetime ($\tau_0 \approx 10^{-8}$ s). If we

use as values, $a = 10^{-7}$ cm, $T_c = 210$ K and $G = 10^{20}$ cm⁻³.s⁻¹, we obtain $L \approx 13$, $\sigma_p / eG = 5.6 \cdot 10^{-11}$ cm²/V which is in well agreement with the calculated $\sigma_p / eG = 3 \cdot 10^{-11}$ cm²/V in the very low temperature region.

5. CONCLUSION

The primary aim of this work was to form a general picture of the electronic properties of a-Si:H to elucidate the transport mechanism. The temperature dependence of the photoconductivity of un-doped a-Si:H was studied in the [30-500 K] temperature range. The experimentally temperature dependence of the photoconductivity is characterized by the following features: the thermal quenching, the low activated region and the temperature independent photoconductivity at very low temperatures. All these observations are well reproduced by the model in un-doped a-Si:H. The interpretation of the model results is through examination of the relative contributions of two processes: the multiple trapping and multiple trapping associated with the hopping process. This allowed us to show firstly that the multiple trapping transport is an important process and the hopping conduction is not significant near the thermal quenching at temperature $T \geq 140$ K. Secondly the relative hopping transport below 140 K has made an important contributions process in the photoconductivity result of a-Si:H. It explains successfully the low activated region and the temperature independent photoconductivity at very low temperatures.

Finally, we can conclude that the multiple trapping model associated with hopping process reproduces well the experimental features mentioned above than the simple multiple trapping model.

REFERENCES

- [1] J.H. Zhou and S.R. Elliott, Phil. Mag. B66, 801, 1992.
- [2] H. Dersch, L. Schweitzer and J. Stuke, Phys. Rev. B28, 4678, 1983.
- [3] P.E. Vanier, A.E. Delahoy and R.W. Griffith, J. Appl. Phys. 52, 5235, 1981.
- [4] A. Vomvas and H. Fritzsche, J. Non-Cryst. Solids 97&98, 823, 1987.
- [5] H. Fritzsche, B.G. Yoon, D.Z. Chi and M.Q. Tran, J. Non-Cryst. Solids 41, 123, 1992.
- [6] F. Vaillant, D. Jousse and J.D. Bruyère, Phil. Mag. B 57, 649, 1988.
- [7] B. Cleve and P. Thomas, Proceeding of MRS spring meeting, San Francisco, 1990.
- [8] J.H. Zhou, S.R. Elliott, Phys. Rev. B 48, 1505, 1993.
- [9] M.Q. Tran, Phil. Mag. B 72, 35 (1995).
- [10] J.G. Simmons and G.W. Taylor, Phys. Rev. B 54, 502, 1971.
- [11] C. Cloude, W.E. Spear, P.G. Lecomber and A.C. Hourd, Phil. Mag. B 54, L113, 1986.
- [12] W.E. Spear and S.C. Cloude, Phil. Mag. B 58, 467, 1988.
- [13] R.E. Johanson, Phys. Rev. B 45, 4089, 1992.
- [14] B.I. Shklovskii, H. Fritzsche and S.D. Baranovskii, Phys. Rev. Lett. 62, 2989, 1989.
- [15] D. Monroe, Phys. Rev. Lett. 54, 146, 1985.
- [16] S.D. Baranovskii, P. Thomas and G.J. Adriaenssens, J. Non-Cryst. Solids 190, 283, 1995.
- [17] K. Winer, Phys. Rev. Lett. 63, 1487, 1989.
- [18] M.J. Powell and S.C. Deane, Phys. Rev. B 48, 10815, 1993.
- [19] M.J. Powell and S.C. Deane, Phys. Rev. B 33, 10121, 1996.
- [20] W.B. Jackson, S.M. Kelso, C.C. Tsai, J.W. Allen and S.J. OH, Phys. Rev. B 31, 5187, 1985.
- [21] C. Longeaud and J.P. Kleider, Phys. Rev. B 48, 8715, 1993.
- [22] J.T. Sheferd, Ph.D, Thesis, University of Abertay Dundee, 1998.
- [23] N.F. Mott and E.A. Davis, 'Electronic Processes in Non-Crystalline Materials', Clarendon Press Oxford, 1979.
- [24] A. Miller and E. Abraham, Phys. Rev. 120, 745, 1960.
- [25] J.M. Marshall, P.G. Lecomber and W.E. Spear, Solid State Comms. 54, 11, 1985.
- [26] S.D. Baranovskii, B. Cleve, R. Hess and P. Thomas, J. Non-Cryst. Solids, Vol. 43, pp. 164-166, 1993.